Chinese Chemical Letters 32 (2021) 13–20

Contents lists available at ScienceDirect

Chinese Chemical Letters

journal homepage: www.elsevier.com/locate/cclet

Review

Recent advances in the improvement of g-C_3N_4 based photocatalytic materials

Yupeng Xing, Xiaoke Wang, Shuhua Hao, Xueli Zhang, Xiao Wang, Wenxuan Ma, Gang Zhao*, Xijin Xu*

School of Physics and Technology, University of Jinan, Ji'nan 250022, China

ARTICLE INFO

Article history:
Received 20 October 2020
Received in revised form 31 October 2020
Accepted 2 November 2020
Available online 4 November 2020

Keywords:
Carbon nitride
Modification
Enhancement
Photocatalyst
Hydrogen evolution reaction

ABSTRACT

g-C_3N_4 have been widely used in the fields of photocatalytic hydrogen production, photocatalytic degradation of dyes and oxidative degradation of toxic gases due to their excellent performance. It has attracted extensive attention in recent years due to its highly efficient photocatalytic capacity of hydrogen generation, water oxidation, carbon dioxide reduction and degradation of organic pollutants. Because of the abundant carbon and nitrogen composition of the earth, large-scale production and industrial applications of this material are possible. The modification of this material makes its performance more excellent so that this new material can obtain a steady stream of vitality. These outstanding works have become important materials and milestones on the road to mankind's photocatalytic hydrogen production. This review will begin with the basic idea of designing, synthesizing and improving g-C_3N_4 based photocatalytic materials, and introduce the latest development of g-C_3N_4 photocatalysts in hydrogen production from four aspects of controlling the carbon/nitrogen ratio, morphology, element doping and heterojunction structure of g-C_3N_4 materials.

1. Introduction

Energy is the cornerstone of the development of modern society [1]. With the continuous advancement of industrialization and urbanization, the demand for fossil energy such as petroleum, coal and natural gas is increasing [2]. The competition for depletable fossil energy resources is gradually escalating into a regional hotspot issue. More and more traditional and non-traditional problems are highlighted: the energy crisis is attracting more and more people's attention, which requires the development of sustainable energy to replace traditional fossil fuels [3]. The need for clean energy is becoming more and more urgent [4]. In the exploration of many alternative energy sources, solar energy is a clean, inexhaustible energy, which is considered to be the most potential and the most environmentally friendly renewable energy source. This is conducive to the sustainable development of the environment and energy [5–7]. In addition to using photovoltaic panels to generate electricity directly, another direction with great development prospects is to develop efficient photocatalysts. The photocatalyst, illuminated by sunlight, absorbs photons from the sun and split water into hydrogen and oxygen [8–15]. It is a simple, environmentally friendly way to deal with our energy issues. It is also a hot topic for scholars in relevant fields to study. The problem is that although various photocatalysts are constantly emerging, their photocatalytic efficiency is not satisfactory: usually less than 1%. However, the photocatalytic efficiency of photocatalysts suitable for industrial applications should be above 10% [16]. Although there is still a long way to go to realize the practical application of industrialization, after so many years of exploration, there are many encouraging achievements in the field of photocatalytic hydrolysis in recent years.

There are many members in the large family of photocatalytic materials, including zero-dimensional granular photocatalytic materials [17,18], one-dimensional linear photocatalytic materials [19–21], two-dimensional layered photocatalytic materials [22–28] and three-dimensional bulk photocatalytic materials [29,30]. Among these photocatalytic materials, g-C_3N_4 have been attracted extensive attention in recent years due to its excellent performance such as highly efficient photocatalytic hydrogen generation, water oxidation (for making hydrogen peroxide), carbon dioxide reduction, organic pollutant degradation and artificial photosynthesis [31–40]. Because the earth is rich in metal-free elements for the synthesis of this photocatalytic material, good photochemical stability, and thermal stability, as well as easy to use synthesis of

* Corresponding authors.
E-mail addresses: sps_zhaog@ujn.edu.cn (G. Zhao), sps_xuxj@ujn.edu.cn (X. Xu).

https://doi.org/10.1016/j.cclet.2020.11.011

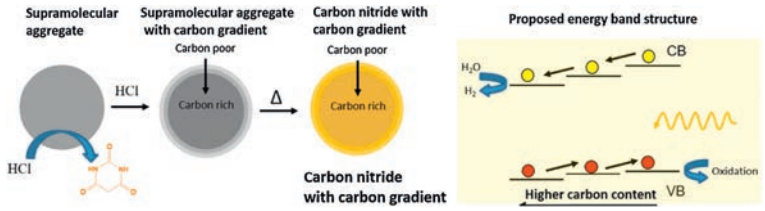

Fig. 1. Graphic representation of the proposed carbon nitride photoactive material from the supramolecular assembly and the corresponding energy-band structure. Reproduced with permission [67]. Copyright 2017, American Chemical Society.

melamine, urea, thiourea, *etc.* [41]. All the above mentioned are the great advantages of this material [42]. However, the bulk g-C_3N_4 obtained after direct calcination of the precursor is always limited by its low specific surface area, high photoexcited electron and hole recombination rate, and limited light absorption in the visible range [43]. Therefore, the modification and optimization of g-C_3N_4 have important guiding significance for the future research direction of photocatalytic hydrogen production.

In 1972, the first year of the era of photocatalysis, Fujishima discovered that water could be decomposed into hydrogen and oxygen by UV irradiation on TiO_2 electrodes [44], thus opening up a new research field: Photocatalysis. After that, people gradually realized that hydrogen and oxygen reacted to form water is an exothermic reaction. Producing hydrogen and oxygen from water is the reverse reaction, which requires a lot of energy from the outside world [45]. Therefore, pure water cannot perform photocatalytic reaction spontaneously under light irradiation, which requires a photocatalyst to drive and convert the scattered solar energy with low energy density into hydrogen energy which is easier to store and high energy density. In order for the photocatalyst to work, the photon energy of incident light must be greater than the band gap of the semiconductor photocatalyst, so that the electrons in the valence band (VB) will be transferred to the conduction band (CB). And then it has holes in VB and electrons in CB. Then these holes and electrons migrate to the surface of the photocatalyst and the redox reaction occurs at the surface-active site of the contact surface between the photocatalyst and water [46].

With the development of photocatalytic materials, people have never stopped their exploration of g-C_3N_4. In the past decades, people have done a lot of work. This review will be from the design and modification of g-C_3N_4 based photocatalytic materials according to these ideas: Change the content of carbon and nitrogen of carbon nitride (CN) material, and change the morphology of CN, element doping and construct heterostructure to introduce the latest methods of CN modification and the development of frontier.

2. Modification strategies of different g-C_3N_4 photocatalytic materials

Graphite phase carbon nitride (g-C_3N_4) is a typical metal-free semiconductor, which has been widely studied due to its excellent applications in H_2 production, environmental remediation, redox and photosynthesis [47–51]. Bulk g-C_3N_4 has thermal stability, chemical stability and photocatalytic stability and can be easily synthesized by direct thermal polymerization of nitrogen-rich precursors [52,53]. However, the photocatalytic efficiency of the directly polymerized g-C_3N_4 material is far from satisfactory, which is due to the limited visible light absorption range, small surface area, limited active site and fast recombination [54–56]. Therefore, in order to improve the photocatalytic performance of g-C_3N_4, morphological construction rate of photogenerated carriers [57,58], construction of Z-scheme heterostructure [59–61], doping of non-metallic or metallic elements [62,63], introducing element defects or vacancies, protonation and other technologies can be used [64–66]. Inspired by two-dimensional graphene-like nanosheets of materials, efforts have also been made to convert bulk g-C_3N_4 into porous structures that compose thin nanosheets that help provide superior photocatalytic activity.

2.1. Adjust the ratio of carbon to nitrogen in g-C_3N_4

2.1.1. Change the carbon concentration

Jesus Barrio *et al.* [67] prepared solutions with different concentration gradients by adding 37% HCl of different volumes to a 1:1:0.1 (molar ratio) solution of cyanuric acid, melamine, barbiturate (Fig. 1, left). Mix with an automatic shaker and centrifuge. The powder was dried overnight at 60 °C in a vacuum furnace and then calcined for 4 h at 550 °C in an atmosphere of nitrogen. This synthesis method does not require any template method or other chemical treatment, but instead uses the intelligent design of supramolecular components to target the photophysical and catalytic properties of carbon nitride. The use of hydrogen-chlorine interactions leads to a carbon gradient through initial supramolecular assembly that can be transferred directly to the final carbonitriding material, thus reinforcing the importance of monomer sequences in the initial precursor. In supramolecular combinations, the rearrangement of monomers leads to the formation of unique energy level structures in the final material (Fig. 1, right), which has been proposed to improve the charge separation efficiency under light and thus the photocatalytic activity, resulting in higher hydrogen production. The photocatalytic efficiency of this material can reach 380 μmol g^{-1} h^{-1}.

2.1.2. Change the nitrogen concentration

Zhuge *et al.* [68] adjusted the electronic structure and energy band level of graphene phase carbon nitride by constructing different nitrogen content. In this way, prepared material has high photocatalytic activity. The team prepared nitrogen-rich CN (CN-NR 100) and nitrogen-deficient CN (CN-ND 500) by adjusting the nitrogen content in the CN material using isonicotinic acid (IA) as a precursor additive. Both materials can provide more photocatalytic sites, and the narrower band gap which can enhance the absorption of visible light and significantly improve the efficiency of carrier separation. Therefore, this material has good photocatalytic hydrogen production rates of 73 μmol g^{-1} h^{-1} (about 4 times of bulk CN) and 120 μmol g^{-1} h^{-1}(about 6 times of bulk CN) respectively. The preparation process of these two materials is shown in Fig. 2.

Although the photocatalytic performance of the materials can be improved by adjusting the carbon to nitrogen ratio of the materials, there are also some problems such as high energy consumption and uneven photocatalytic materials. In addition, the photocatalytic efficiency improved by simple regulation of C-N ratio is very limited, and the hydrogen production efficiency is still very low. Therefore, this method limits the practical application of photocatalyst.

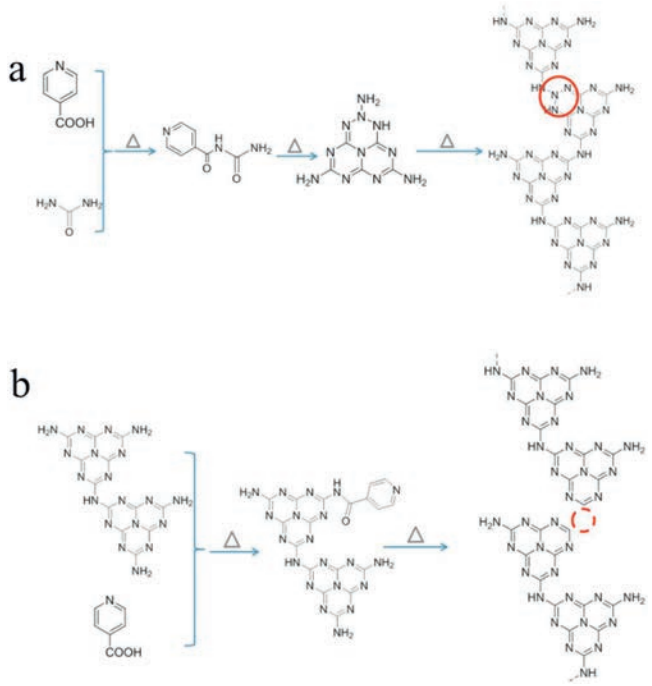

Fig. 2. (a) Synthesis process of nitrogen-rich CN and (b) nitrogen-deficient CN. Reproduced with permission [68]. Copyright 2018, Wiley-VCH.

2.2. Different structures were constructed to enhance the photocatalytic performance

The microstructure of materials, like two-dimensional materials, has a great influence on their properties [69–73]. Among two-dimensional photocatalyst preparation methods, thermal etching in air [74], ultrasonic stripping in various solutions [75–80] and GQDs-Assistant exfoliation [81] were used. To date, there have been many attempts to improve the photocatalytic performance of carbon nitride materials by changing their structure. Common means are: larger material through some ways (ultrasound processing) to tear into smaller pieces; by calcination and other means, the two-dimensional material is curled to form a tube; by making vacancy porous structure is prepared and even grow into other peculiar geometric structures. For example, nanospheres [82].

2.2.1. Aerogel structure

Zhang *et al.* [83] prepared aerogels composed of self-supporting carbon nitride nanolayer by a simple method combining hydrothermal condensation and thermal stripping. The curved nanosheets is easy to self-support. We can clearly see the microstructure of this material through SEM (Figs. 3a-d). The structure is so light that it can be placed on the stamens of a flower (Fig. 3b insert). It can maintain the specific surface and avoid aggregation; sufficient nitrogen vacancy makes the carbon nitride aerogels more effective than the bulk carbon nitride aerogels in catalyzing hydrogen evolution reaction. Self-supported aerogels composed of carbon nitride nanofilms can be used as bifunctional photocatalysts. Due to the large surface area and nitrogen vacancy, the photoreduction and photooxidation properties of aerogels are enhanced. The catalytic hydrogen production rate of carbon nitride aerogel was close to 4.2 mmol g^{-1} h^{-1} (Fig. 3f). It is worth noting that compared with traditional carbon-based photocatalysts, carbon-based aerogels show excellent performance in photocatalysis. Through density functional theory and experimental

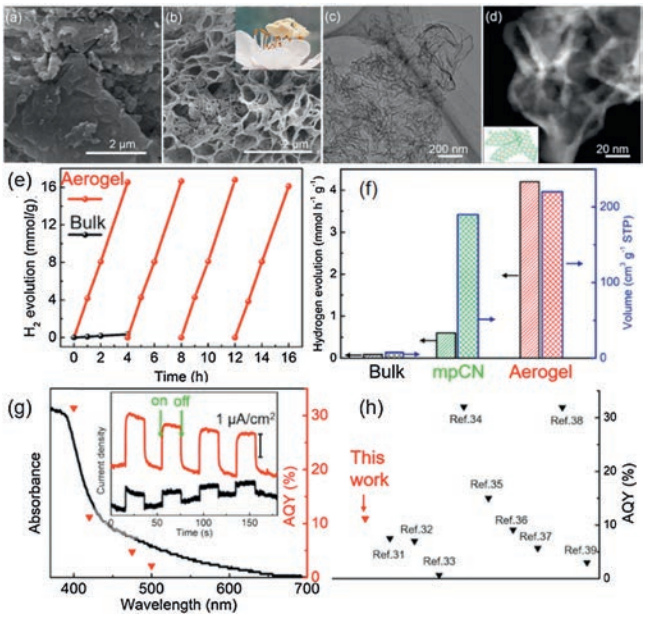

Fig. 3. (a) SEM image of carbon nitride aerogel. (b) TEM image of carbon nitride aerogel. (c) STEM image of carbon nitride aerogel acquired in the HAADF mode. (d) The self-supported entangled nanolayers of the carbon nitride aerogel. (e) Typical time course of H_2 production of carbon nitride aerogel and bulk carbon nitride under visible-light irradiation ($\lambda > 420$ nm). (f) Hydrogen evolution rate comparison of carbon nitride aerogel and control samples. (g) AQY values under different monochromatic light irradiation and UV–vis spectra of carbon nitride aerogel. (h) AQY comparison of carbon nitride aerogel. Reproduced with permission [83]. Copyright 2019, American Chemical Society.

results, it is proved that the introduction of nitrogen vacancy in carbon nitride leads to the formation of curved aerogel structure.

2.2.2. Porous g-C_3N_4 nanosheet

Huang *et al.* [84] found an exciting, pre-designed non-template precursor (melamine) pretreatment scheme to achieve higher efficient photocatalytic reduction and oxidation of porous g-C_3N_4 nanosheets. During the hydrothermal pretreatment, thiourea solution was introduced to etch the surface of melamine, and porous g-C_3N_4 nanosheets were created (Fig. 4a). The microstructure and porosity of g-C_3N_4 can be adjusted only by controlling the thiourea dosage. The obtained porous g-C_3N_4 nanosheets not only

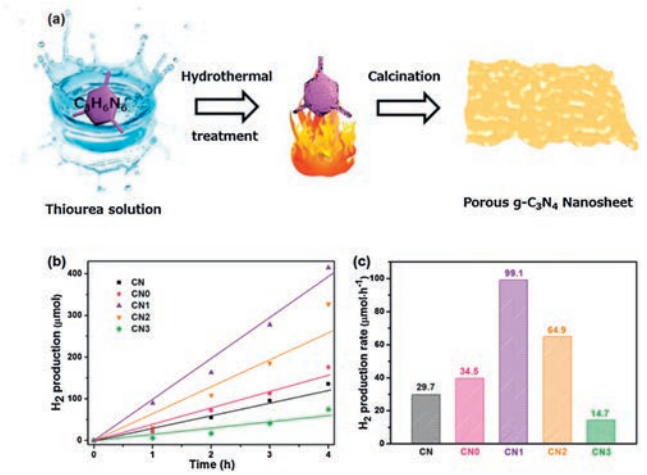

Fig. 4. (a) The preparation of porous g-C_3N_4 nanosheet. (b) Photocatalytic H_2 production curves. (c) H_2 production rate of CN with different thiourea dosage under visible light. Reproduced with permission [84]. Copyright 2017, Royal Society of Chemistry.

increase the specific surface area, but also enhance the light absorption in the visible region. This work demonstrated by systematic characterization of charge behavior (transient photocurrent, linear scanning volt-amperes, electrochemical impedance spectroscopy, photoluminescence, and surface photovoltage spectroscopy) that the porous nanosheet structure significantly enhanced the separation of photocarriers. Compared with bulk g-C_3N_4 material, the visible photocatalytic performance of porous g-C_3N_4 nanosheets in hydrogen evolution was significantly enhanced (about 3.3 times shown in Figs. 4b and c). The separation of photoelectrons from vacancies can be effectively promoted. For these reasons, the visible light catalytic hydrogen evolution performance of porous g-C_3N_4 was significantly enhanced.

2.2.3. Nanowires

Ultra-long carbon nitride nanostructures have a high aspect ratio and a high surface-volume ratio, making them suitable for a variety of applications such as photocatalysts, water pollution degradation and sensors. Barrio *et al.* [85] reported the synthesis of carbon nitride filaments with a horizontal size of 4 cm using unique supramolecular spheres and graphitized carbon nitride (g-C_3N_4) monomer as reactants (Fig. 5b). The chemical structure of the supramolecular sphere and the growth process of nanowires are shown in Fig. 5a. The study by atomic scanning electron microscope showed that the g-C_3N_4 nanowires spontaneously began to grow from the sphere through roasting, in which the carbon nitride sphere was used as the substrate for growth. The material will spontaneously complete the rest of the assembly. Interestingly, nanowires grow differently at different temperatures (Fig. 5c). The carbon-rich g-C_3N_4 porous membrane is assembled. Nanofibers with different morphology, chemical composition and electronic properties can be excellent photocatalysts. g-C_3N_4 nanowires exhibit excellent photocatalytic activity in hydrogen production. This work provides an idea for the design of g-C_3N_4 nanostructures and materials for photocatalytic applications.

2.2.4. Nano-fragments

Vu *et al.* [86] modified the structure of bulk g-C_3N_4 with high-pressure atmosphere containing NH_3 and H_2O formed by condensation polymerization of urea. In the process of modification, bulk g-C_3N_4 was put into the reactor containing urea and heated to 205 °C for 36 h (The synthesis process is shown in Fig. 6c). The condensation of urea produces NH_3 and water vapor. These reactions maintain an extremely high pressure in the reactor. Under high pressure, the carbon nitride skeleton was fractured into nanosheets. The photocatalytic hydrogen production efficiency of this material is 2598 $\mu mol\, g^{-1}\, h^{-1}$ (Figs. 6a and b).

Photocatalysts with various morphologies have obvious advantages. For example, two-dimensional photocatalysts obtained by specific means have larger specific surface area and more reactive sites. Other elements introduced during the construct process can also play a decorative role. However, there are still some problems such as strict requirement on reaction temperature and uneven particle size of synthetic materials.

2.3. Element doping

Element doping is an effective strategy to adjust the band structure of photocatalysts and expand the light absorption region [87]. It has been widely used to adjust the optical absorption of internal bandgap structure by using non-metallic (B, O, S, I) doped g-C_3N_4 and to adjust the photocatalytic performance of g-C_3N_4 to promote the redox potential in visible light [88–92]. However, due to the quantum confinement effect that increases the band gap, the light absorption range of nanosheets generally decreases [93,94]. Therefore, we can use elemental doping to adjust the band structure of g-C_3N_4, which can not only increase light absorption, but also improve charge separation [95]. The following reports will be made from oxygen doping, boron doping, phosphorus doping and halogen doping.

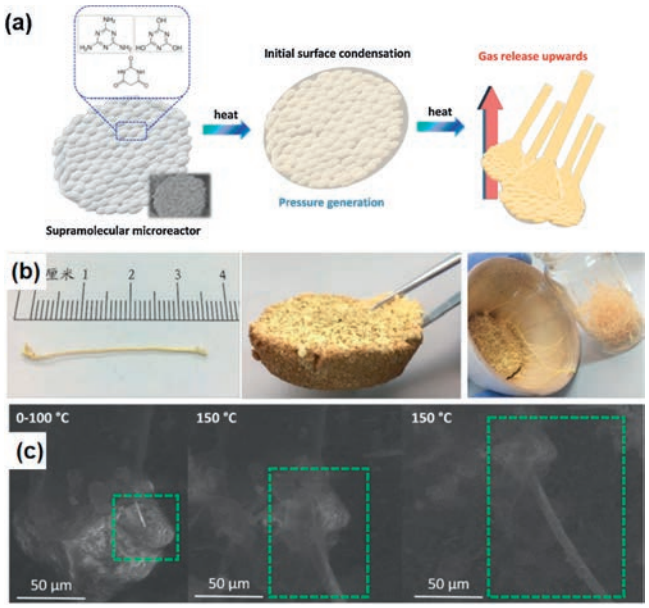

Fig. 5. (a) The preparation of carbon nitride nanowires. (b) Images of a 4 cm free-standing g-C_3N_4 filaments. (c) *In situ* heating SEM images at different temperatures. Reproduced with permission [85]. Copyright 2018, American Chemical Society.

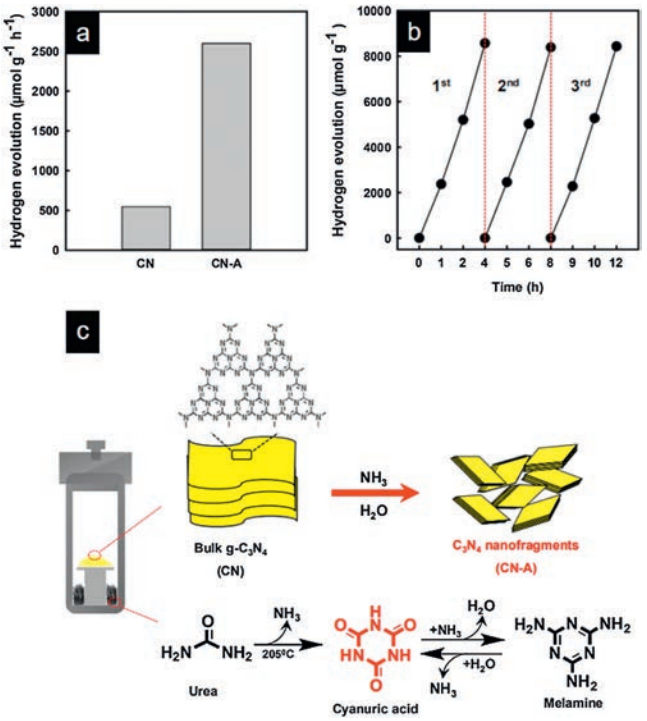

Fig. 6. (a) H_2 production rate of CN and CN fragments samples and (b) H_2 production of CN fragments for three cycles. (c) The preparation of CN nanofragments. Reproduced with permission [86]. Copyright 2019, American Chemical Society.

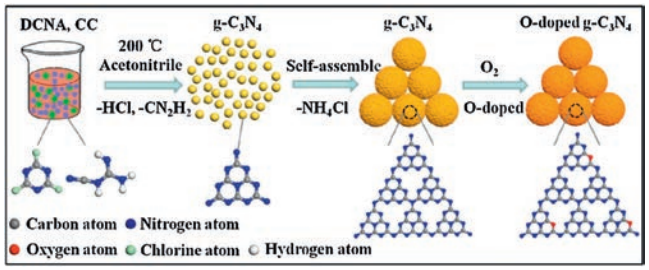

Fig. 7. The preparation of oxygen-doped g-C_3N_4 nanospheres. Reproduced with permission [96]. Copyright 2018, Royal Society of Chemistry.

2.3.1. Oxygen doping

Wei *et al.* [96] greatly improved photocatalytic performance by doping oxygen in g-C_3N_4. The preparation of oxygen-doped g-C_3N_4 nanospheres is shown in Fig. 7. The amount of oxygen doping can be controlled by the copolymerization of the precursor. Therefore, oxygen-doped g-C_3N_4 showed excellent photocatalytic performance, with rhodamine B visible light degradation rate of 0.249 min^{-1} and hydrogen evolution rate of 3174 $\mu mol\, g^{-1}\, h^{-1}$, which were both 35 times and 4 times higher than the traditional g-C_3N_4. Zhang *et al.* [97] also doped different oxygen element concentrations by adding different proportions of oxalic acid to common carbon nitride materials. The efficiency of photocatalysis is improved effectively. The introduction of oxygen element can adjust the energy band structure and increase the absorption of visible light. These works provide new ways for the rational design and preparation of O doped g-C_3N_4 photocatalyst for the production of H_2.

2.3.2. Boron doping

Thaweesak *et al.* [98] prepared a new type of boron-doped graphitic carbon nitride nanometer material by one-pot thermal condensation. It is found that the best time catalytic hydrogen evolution activity is 1880 $\mu mol\, g^{-1}\, h^{-1}$ ($\lambda > 400$ nm), more than 12 times larger than bulk g-C_3N_4. The high photocatalytic performance is attributed to the combination of band structure construction and morphological control. By using sodium borohydride corrosion, He *et al.* [99] successfully doped boron into a line-shaped carbon nitride photocatalytic material. The photocatalytic performance was improved successfully. Boron doping not only reduces the band gap and absorbs more visible light, but also has a higher surface area than bulk g-C_3N_4, which greatly improves the photocatalytic performance. These works demonstrate two different synergistic strategies for the preparation of highly efficient non-metallic doped g-C_3N_4 materials.

2.3.3. Phosphorus doping

Kumar *et al.* [100] synthesized phosphorus-doped carbon nitride quantum dots (CNPQDs) through solid thermal condensation of urea, citric acid and 1-butyl-3-methylimidazolium hexafluorophosphate (BMIM-PF_6) in a reactor at 200 °C. The synthesis of carbon nitride doped quantum dots (CNPQDs) is shown in Fig. 8a. In this synthesis process, urea and citric acid generate basic carbonitride skeleton by condensation polymerization, and BMIM-PF_6 acts as a phosphorus doping source. Steady state photoluminescence (PL) spectrum of phosphorus doped carbon nitride quantum dots (CNPQDs) and carbon nitride quantum dots (CNQDs) in water is shown in Fig. 8b. ^{15}N and ^{31}P CPMAS NMR spectra of CNPQDs is shown in Fig. 8c. The process of (CNPQDs) modification in titanium dioxide array is shown in Figs. 8d and e.

2.3.4. Halogen doping

Iodine doping: In this study, Iqbal *et al.* [101] prepared a nano-mesoporous g-C_3N_4 doped with iodine and N vacancy simultaneously by a direct one-step method. In particular, the simultaneous heating of glucose and NH_4I has shown some interesting phenomena, such as synergistic iodine-doped mesoporous g-C_3N_4 epidermoid shedding and the introduction of N vacancy due to the release of nitrogen-rich gas. In this work, the synthesized iodine-doped mesoporous g-C_3N_4 has an excellent photocatalytic hydrogen production performance up to 7819.2 $\mu mol\, g^{-1}\, h^{-1}$ under simulated solar light, which is nearly 6.5 times higher than the bulk g-C_3N_4 and other kinds of iodine-doped g-C_3N_4 photocatalysts. This work presents a simple and feasible way to synthesize high

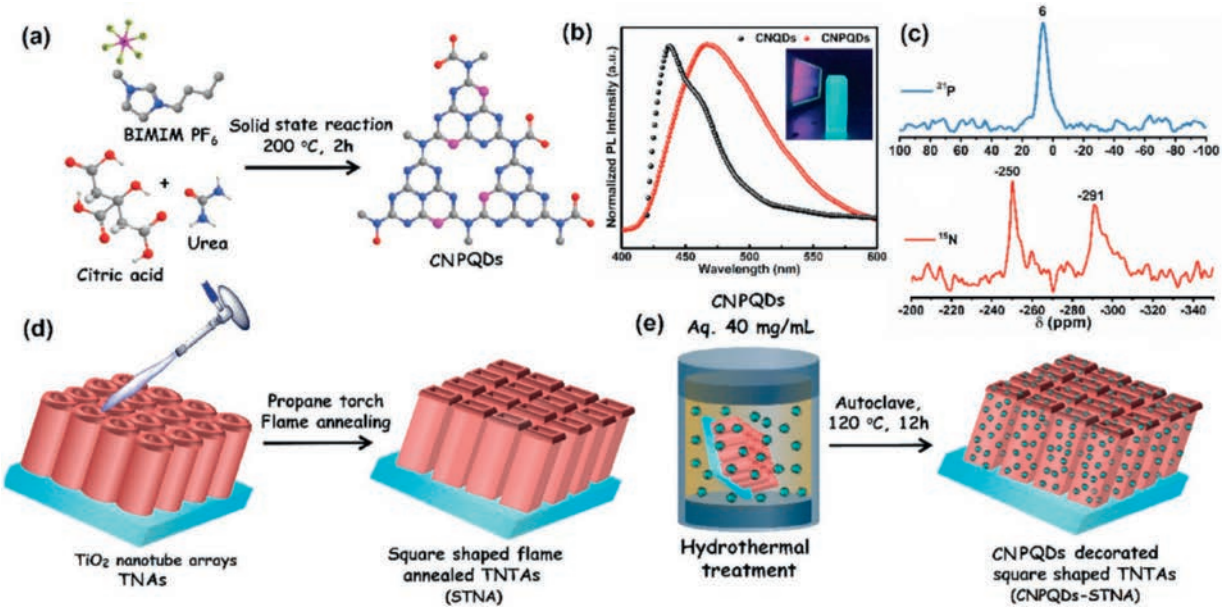

Fig. 8. (a) Schematic diagram illustrating the synthesis of phosphorus doped carbon nitride quantum dots (CNPQDs). (b) Steady state PL spectrum of CNPQDs and carbon nitride quantum dots (CNQDs) in water. Inset showing fluorescence of CNPQDs sample under UV light irradiation. (c) N and P CPMAS NMR spectra of CNPQDs. (d-f) The preparation of CNPQDs decorated square shaped TNTAs. Reproduced with permission [100]. Copyright 2019, Wiley-VCH.

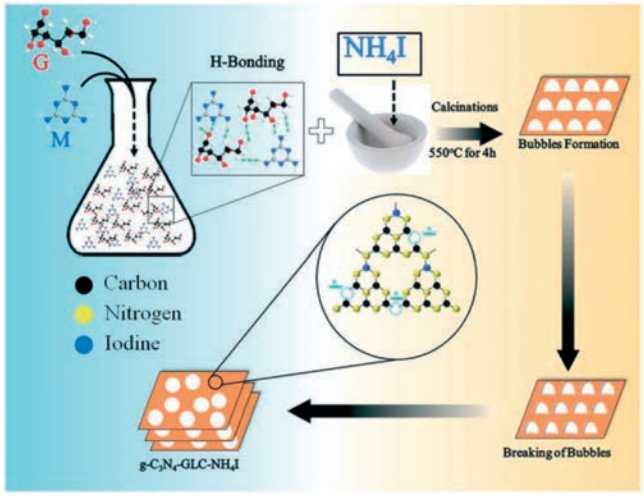

Fig. 9. Schematic of synthesizing N-vacant iodine doped mesoporous g-C_3N_4 nanosheets. Reproduced with permission [101]. Copyright 2019, Royal Society of Chemistry.

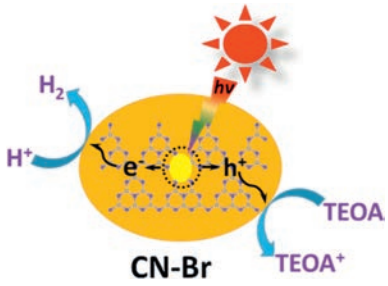

Fig. 10. Photocatalytic mechanism of CN-Br photocatalyst. Reproduced with permission from [102]. Copyright 2016, Elsevier.

performance metal-free g-C_3N_4 photocatalyst by changing electronic transition through reasonable band structure construction. The carbon nitride process modified by iodine is shown in Fig. 9.

Bromine doping: Lan *et al.* [102] proposed a bromide doped graphite phase carbon nitride method. Bromine modification can improve the optical, conductance and photocatalytic properties of g-C_3N_4 while keeping the core structure of Triazine as the main component of the material. Photocatalytic mechanism of CN-Br photocatalyst is shown in Fig. 10. The modification method is generally applicable to several precursors of g-C_3N_4, including urea, dicyandiamide, ammonium thiocyanate and thiourea. This work also provides a feasible modification way for the rational design and synthesis of g-C_3N_4-based photocatalyst.

The catalytic performance, especially that of visible light, can be improved effectively by element doping. However, it still has some disadvantages that cannot be ignored: for example, the preparation process is complicated, the production cost is increased and industrial production is limited.

2.4. Construct heterojunctions

Heterostructure photocatalysts can be divided into two types according to the photoelectron-hole migration mode: A class of heterogeneous junction photocatalysts, dominated by classical carrier transfer, is composed of wide band gap photocatalyst and narrow band gap photocatalyst [103–108]. CB of narrow band gap material has a higher energy level and a wider spectral absorption range of narrow band gap material, which can effectively widen the width of response spectrum of heterojunction structure

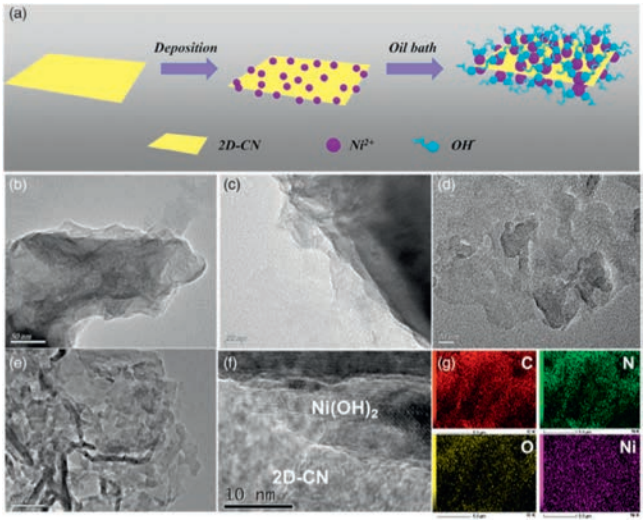

Fig. 11. (a) The formation process of $Ni(OH)_2$/2D-CN nanohybrids. (b,c) TEM images of the $Ni(OH)_2$. (d) 2D-CN, (e,f) 0.25 $Ni(OH)_2$/2D-CN nanohybrids and (g) element mappings for C, N, O and Ni. Reproduced with permission [119]. Copyright 2019, Wiley-VCH.

material. The wide band gap semiconductor has relatively low conduction band energy level, which makes the photoelectrons of the narrow band gap photocatalyst material transferred to the CB of the wide band gap material, thus generating a large number of photoelectrons and significantly improving the photocatalytic activity [109]. The other is heterojunction photocatalytic materials with Z-strategy carrier migration as the main stream, on the condition that the top of a semiconductor's VB is higher than that of the other conductor's CB [110–118]. When carriers pass through the control interface, lower energy photogenic carriers are directly recombined to leave higher energy photogenic carriers, thus achieving higher photocatalytic performance.

Hao *et al.* [119] improved the performance of photocatalytic hydrogen evolution by using $Ni(OH)_2$ as the operational synergetic catalyst for ultra-fine combination with 2D-CN to form 2D/2D heterojunctions. The preparation process is shown in Fig. 11a. Due to the high mobility of $Ni(OH)_2$ holes and the unique 2D/2D heterogeneous junction of $Ni(OH)_2$/2D-CN, the specific photocatalyst $Ni(OH)_2$/2D-CN accelerates the separation/transport of photocarriers, thus achieving a breakthrough in continuous photocatalytic hydrogen evolution without the use of Pt co-catalyst and sacrificial agent. We can clearly see through TEM images: $Ni(OH)_2$ (Figs. 11b and c), 2D-CN (Fig. 11d) and 0.25 $Ni(OH)_2$/2D-CN nanohybrid (Figs. 11e and f). In this work, 10% triethanolamine was used as sacrificial agent, and the hydrogen evolution rate of $Ni(OH)_2$/2D-CN at 400 nm was 921.4 $\mu mol\ g^{-1}\ h^{-1}$, and the external quantum efficiency (EQE) was 5.21%. This work provides a new way to explore new photocatalytic materials.

3. Conclusion and perspective

Up to now, g-C_3N_4 as a metal-free, visible light responsive photocatalyst, is still a research hotspot in hydrogen production field. In this review, the preparation progress and catalytic effect of g-C_3N_4-based composites are reviewed from four aspects: adjusting the carbon/nitrogen ratio of materials, synthesizing different morphologies, element doping and constructing heterogeneous structures. Through people's constant exploration, there has been great progress. However, the g-C_3N_4-based photocatalysts

currently used for integral water separation are still far from the optimal level for sustained hydrogen production from water. Using semiconductor photocatalysts to achieve solar-powered water cracking to produce highly efficient hydrogen remains a challenge. We need to develop more effective photocorrosion protection on g-C_3N_4-based catalysts and construct new and more effective co-catalysts to improve photocatalytic activity and stability. The photocatalytic properties can be improved by modifying CN materials as mentioned above. This review provides reference for further improvement of photocatalyst materials.

Declaration of competing interest

We declare that we do not have any commercial or associative interest that represents a conflict of interest in connection with the work submitted.

Acknowledgments

This work was supported by the National Natural Science Foundation of China (Nos. 51672109, 51802177), the Independent Cultivation Program of Innovation Team of Ji'nan City (No. 2019GXRC011), and Natural Science Foundation of Shandong Province (No. ZR2018BEM019). All the authors discussed the results and commented on the manuscript.

References

[1] S. Sen, S. Ganguly, A. Das, J. Sen, S. Dey, J. Afr. Earth Sci. 122 (2016) 25–31.
[2] B.H. Kreps, Am. J. Econ. Sociol. 79 (2020) 695–717.
[3] G. Zhao, H.C. Yang, M.Q. Liu, X.J. Xu, Front. Chem. 6 (2018) 551.
[4] H.J. Maaß, H.O. Möckel, Chem. Eng. Technol. 43 (2020) 111–118.
[5] Z. Wang, C. Li, K. Domen, Chem. Soc. Rev. 48 (2019) 2109–2125.
[6] P. Yu, L.V. Besteiro, Y. Huang, et al., Adv. Opt. Mater. 7 (2019) 1800995.
[7] J.D. Xiao, H.L. Jiang, Acc. Chem. Res. 52 (2019) 356–366.
[8] G. Zhao, A. Wang, W. He, Y. Xing, X. Xu, Adv. Mater. Interfaces 6 (2019) 1900062.
[9] X. Ling, Y. Xu, S. Wu, et al., Sci. China Chem. 63 (2020) 386–392.
[10] A. Hayat, N. Shaishta, S.K.B. Mane, et al., J. Colloid Interface Sci. 560 (2020) 743–754.
[11] K.M. Alam, P. Kumar, P. Kar, et al., Nanotechnology 31 (2020) 84001.
[12] S. Wang, H. Zhao, X. Zhao, et al., Chem. Eng. J. 381 (2020) 122593.
[13] Z. Qin, Z. Huang, M. Wang, et al., Appl. Catal. B: Environ. 261 (2020) 118211.
[14] Z. Liang, G. Ba, H. Li, N. Du, W. Hou, J. Alloys Compd. 815 (2020) 152488.
[15] Z. Mo, X. She, Z. Chen, et al., Chemcatchem 12 (2020) 1169–1176.
[16] S.S. Chen, T. Tsuyoshi, D. Kazunari, Nat. Rev. Mater. 2 (2017) 17050.
[17] F. Raziq, J. He, J. Gan, et al., Appl. Catal. B: Environ. 270 (2020) 118870.
[18] Q. Liu, C. Zeng, Z. Xie, et al., Appl. Catal. B: Environ. 254 (2019) 443–451.
[19] K. Sielicki, M. Aleksandrzak, E. Mijowska, Appl. Surf. Sci. 508 (2020) 145144.
[20] S. Zhao, J. Fang, Y. Wang, Y. Zhang, Y. Zhou, ACS Sustain. Chem. Eng. 7 (2019) 10095–10104.
[21] Y. Xin, Y. Huang, K. Lin, Y. Yu, B. Zhang, Sci. Bull. 63 (2018) 601–608.
[22] L. Kong, J. Yan, S. Liu, ACS Sustain. Chem. Eng. 7 (2019) 1389–1398.
[23] Y. Wang, J. Mao, X. Meng, et al., Chem. Rev. 119 (2019) 1806–1854.
[24] Y. Tu, P. Ren, D. Deng, X. Bao, Nano Energy 52 (2018) 494–500.
[25] Y. Xia, B. Cheng, J. Fan, J. Yu, G. Liu, Sci. China Mater. 63 (2020) 552–565.
[26] G. Zhao, Y. Cheng, Y. Wu, X. Xu, X. Hao, Small 14 (2018) 1704138.
[27] X. Huang, Z. Wu, H. Zheng, W. Dong, G. Wang, Green Chem. 20 (2018) 664–670.
[28] N. Meng, W. Zhou, Y. Yu, Y. Liu, B. Zhang, ACS Catal. 9 (2019) 10983–10989.
[29] W. Yu, T. Zhang, Z. Zhao, Appl. Catal. B: Environ. 278 (2020) 119342.
[30] G. Lu, X. Huang, Y. Li, et al., J. Energy Chem. 43 (2020) 8–15.
[31] M. Zhou, Z. Chen, P. Yang, et al., Appl. Catal. B: Environ. 276 (2020) 118916.
[32] W. Ren, J. Cheng, H. Ou, et al., J. Catal. 389 (2020) 636–645.
[33] Y. Wang, P. Du, H. Pan, et al., Adv. Mater. 31 (2019) 1807540.
[34] G. Liu, S. Yan, L. Shi, L. Yao, Front. Chem. 7 (2019) 639.
[35] Y. Yang, M. Wu, X. Zhu, et al., Chin. Chem. Lett. 30 (2019) 2065–2088.
[36] Q. Liu, F. Wang, Y. Jiang, et al., Carbon 170 (2020) 199–212.
[37] J. Wang, Y. Wang, W. Wang, et al., Chem. Eng. J. 383 (2020) 123193.
[38] J. Shi, L. Mao, C. Cai, et al., Catal. Sci. Technol. 10 (2020) 5896–5902.
[39] L. Lin, Z. Lin, J. Zhang, et al., Nat. Catal. 3 (2020) 649–655.
[40] Y. Zhu, J. Li, J. Cao, et al., APL Mater. 8 (2020) 41108.
[41] Y. Fang, X. Fu, X. Wang, ACS Mater. Lett. 2 (2020) 975–980.
[42] R.P. Liang, L.D. Yu, Y.J. Tong, et al., Chem. Commun. 54 (2018) 14001–14004.
[43] Y. Gao, K. Qian, B. Xu, et al., RSC Adv. 10 (2020) 32652–32661.
[44] L. Finegold, L.C. Jesse, Nature 238 (1972) 38–40.
[45] M.G. Walter, L.W. Emily, R.M. James, et al., Chem. Rev. 110 (2010) 6446–6473.
[46] Q. Liu, L. Wei, Q. Xi, Y. Lei, F. Wang, Chem. Eng. J. 383 (2020) 123792.
[47] D.F. Lv, R.F. Shi, Y.W. Chen, et al., Ind. Eng. Chem. Res. 57 (2018) 12215–12224.
[48] N. Zhang, C. Chen, Y.L. Chen, et al., ACS Appl. Energy Mater. 1 (2018) 2016–2023.
[49] S. Sun, S. Liang, Nanoscale 9 (2017) 10544–10578.
[50] Q. Han, N. Chen, J. Zhang, L. Qu, Mater. Horiz. 4 (2017) 832–850.
[51] N.-A. Mohamed, H. Ullah, J. Safaei, et al., J. Phys. Chem. C 123 (2019) 9013–9026.
[52] L. Jing, D. Wang, Y. Xu, et al., J. Colloid Interface Sci. 566 (2020) 171–182.
[53] B. Antil, L. Kumar, K.P. Reddy, C.S. Gopinath, S. Deka, ACS Sustain. Chem. Eng. 7 (2019) 9428–9438.
[54] B. Antil, R. Ranjan, C.S. Gopinath, S. Deka, J. Mater. Chem. 8 (2020) 13328–13339.
[55] Y. Zheng, Y. Chen, L. Wang, et al., Dalton Trans. 49 (2020) 7598–7604.
[56] B. Yan, Z. Chen, Y. Xu, Chem. Asian J. 15 (2020) 2329–2340.
[57] C. Zhao, G. Tan, J. Huang, W. Yang, H. Ren, A. Xia, ACS Appl. Mater. Interfaces 7 (2015) 23949–23957.
[58] S. Patnaik, S. Martha, K.M. Parida, RSC Adv. 6 (2016) 46929–46951.
[59] R. Bhosale, S. Jain, C.P. Vinod, S. Kumar, S. Ogale, ACS Appl. Mater. Interfaces 11 (2019) 6174–6183.
[60] L. Tang, X. Ouyang, B. Peng, et al., Nanoscale 11 (2019) 12198–12209.
[61] Y. Shen, Q. Han, J. Hu, et al., ACS Appl. Energy Mater. 3 (2020) 6561–6572.
[62] G. Liao, Y. Gong, L. Zhang, et al., Energy Environ. Sci. 12 (2019) 2080–2147.
[63] N. Wang, J. Wang, J. Hu, et al., ACS Appl. Energy Mater. 1 (2018) 2866–2873.
[64] L. Lu, X. Xu, K. An, Y. Wang, F. Shi, ACS Sustain. Chem. Eng. 6 (2018) 11869–11876.
[65] W. Iqbal, B. Yang, X. Zhao, et al., Catal. Sci. Technol. 10 (2020) 549–559.
[66] W. Li, Z. Guo, L. Jiang, et al., Chem. Sci. 11 (2020) 2716–2728.
[67] J. Barrio, L. Lin, X. Wang, M. Shalom, ACS Sustain. Chem. Eng. 6 (2018) 519–530.
[68] G. Zhuge, W. Zhang, ChemCatChem 11 (2018) 1045–1056.
[69] M. Xiao, Z. Wang, M. Lyu, et al., Adv. Mater. 31 (2019) 1801369.
[70] W. Liu, Z. Zhang, D. Zhang, et al., RSC Adv. 10 (2020) 28848–28855.
[71] C. Yao, A. Yuan, Z. Wang, et al., J. Mater. Chem. 7 (2019) 13071–13079.
[72] C. Yao, R. Wang, Z. Wang, et al., J. Mater. Chem. 7 (2019) 27547–27559.
[73] Z. Wang, H. Yu, Y. Xiao, et al., Chem. Eng. J. 394 (2020) 12501.
[74] P. Niu, L. Zhang, G. Liu, H.M. Cheng, Adv. Funct. Mater. 22 (2012) 4763–4770.
[75] X. Zhang, X. Xie, H. Wang, J. Zhang, B. Pan, Y. Xie, J. Am. Chem. Soc. 135 (2013) 18–21.
[76] S. Yang, Y. Gong, J. Zhang, et al., Adv. Mater. 25 (2013) 2452–2456.
[77] J. Xu, L. Zhang, R. Shi, Y. Zhu, J. Mater. Chem. 1 (2013) 14766–14772.
[78] F. Cheng, H. Wang, X. Dong, Chem. Commun. 51 (2015) 7176–7179.
[79] F. Cheng, J. Yan, C. Zhou, et al., J. Colloid Interfaces Sci. 468 (2016) 103–109.
[80] J. Yan, X. Han, J. Qian, et al., J. Mater. Sci. 52 (2017) 13091–13102.
[81] J. Qian, J. Yan, C. Shen, et al., J. Mater. Sci. 53 (2018) 12103–12114.
[82] S. Han, L. Yu, H. Zhang, et al., ChemCatChem 11 (2019) 6203–6207.
[83] B. Zhang, T.J. Zhao, H.H. Wang, ACS Appl. Mater. Interfaces 11 (2019) 34922–34929.
[84] H. Huang, K. Xiao, N. Tian, et al., J. Mater. Chem. 5 (2017) 17452–17463.
[85] J. Barrio, M. Shalom, ACS Appl. Mater. Interfaces 10 (2018) 39688–39694.
[86] N.N. Vu, S. Kaliaguine, T.O. Do, ACS Sustain. Chem. Eng. 8 (2020) 853–863.
[87] W. Wang, J.C. Yu, Z. Shen, D.K.L. Chan, T. Gu, Chem. Commun. 50 (2014) 10148–10150.
[88] K. Ding, L. Wen, M. Huang, et al., Phys. Chem. Chem. Phys. 18 (2016) 19217–19226.
[89] M.Z. Rahman, K. Davey, S.Z. Qiao, J. Mater. Chem. 6 (2018) 1305–1322.
[90] F. Su, C. Xu, Y. Yu, W. Zhang, ChemCatChem 8 (2016) 3527–3535.
[91] H. Zhang, X. Han, H. Yu, Y. Zou, X. Dong, Sep. Purif. Technol. 226 (2019) 128–137.
[92] W. Che, W. Cheng, T. Yao, et al., J. Am. Chem. Soc. 139 (2017) 3021–3026.
[93] K. Hu, M. Yao, Z. Yang, et al., Nanoscale 12 (2020) 12300–12307.
[94] G. Xu, Z. Wang, Q. Liu, et al., ChemistrySelect 4 (2019) 13064–13070.
[95] Q. Wan, F. Wei, Z. Ma, M. Anpo, S. Lin, Adv. Theory Simul. 2 (2019) 1800174.
[96] F. Wei, Y. Liu, H. Zhao, et al., Nanoscale 10 (2018) 4515–4522.
[97] G. Zhang, C. He, P. Zhang, H. Mi, Appl. Catal. B Environ. 283 (2020) 119636.
[98] S. Thaweesak, S. Wang, M. Lyu, et al., Dalton Trans. 46 (2017) 10714–10720.
[99] F. He, S. Wang, H. Zhao, et al., Appl. Surf. Sci. 485 (2019) 70–80.
[100] P. Kumar, P. Kar, A.P. Manuel, et al., Adv. Opt. Mater. 8 (2020) 1901275.
[101] W. Iqbal, B. Yang, X. Zhao, et al., Catal. Sci. Technol. 10 (2020) 549–559.
[102] Z.-A. Lan, G. Zhang, X. Wang, Appl. Catal. B: Environ. 192 (2016) 116–125.
[103] N. Lu, X. Yan, H. Kobayashi, et al., Appl. Catal. B: Environ. 279 (2020) 119378.
[104] S. Wang, L. Chen, X. Zhao, et al., Appl. Catal. B: Environ. 278 (2020) 119312.
[105] H. Jiang, C. Zang, Y. Zhang, et al., Catal. Sci. Technol. 10 (2020) 5964–5972.
[106] L. Chen, Y. Wang, C. Wu, et al., Nanoscale 12 (2020) 13484–13490.
[107] E.D. Koutsouroubi, I. Vamvasakis, I.T. Papadas, et al., ChemPlusChem 85 (2020) 1366–1366.
[108] L. Liu, X. Song, X. Kong, Q. Duan, E. Zhu, RSC Adv. 10 (2020) 9116–9125.
[109] Y. Tian, H. Wang, H. Li, et al., J. Mater. Chem. A 8 (2020) 4647–4676.
[110] C. Jiang, H. Wang, Y. Wang, H. Ji, Appl. Catal. B Environ. 277 (2020) 119235.

[111] H. Shen, M. Wang, X. Zhang, et al., Fuel 280 (2020) 118618.
[112] H. Zhang, G. Tang, X. Wan, J. Xu, H. Tang, Appl. Surf. Sci. 530 (2020) 147234.
[113] M. Jourshabani, B.K. Lee, Z. Shariatinia, Appl. Catal. B: Environ. 276 (2020) 119157.
[114] H. Salari, Mater. Res. Bull. 131 (2020) 110979.
[115] F. Yang, Q. Zhang, J. Zhang, et al., Appl. Catal. B: Environ. 278 (2020) 119290.
[116] Z. Zhao, B. Shen, Z. Hu, et al., J. Hazard. Mater. 400 (2020) 123236.
[117] G. Di, Z. Zhu, H. Zhang, et al., Chem. Eng. J. 401 (2020) 126061.
[118] G. Zhao, S. Hao, J. Guo, et al., J. Catal. 42 (2021) 501–509.
[119] Q. Hao, Y. Song, Z. Mo, et al., Sol. RRL 4 (2020) 1900538.